Peritubular capillaries are rarefied in congenital nephrotic syndrome of the Finnish type

Anne Kaukinen[1], Irmeli Lautenschlager[2], Heikki Helin[3], Riitta Karikoski[3] and Hannu Jalanko[1]

[1]Hospital for Children and Adolescents and Biomedicum Helsinki, University of Helsinki, Helsinki, Finland; [2]Department of Virology, HUSLAB, Helsinki University Central Hospital and University of Helsinki, Helsinki, Finland and [3]Department of Pathology, University of Helsinki, Helsinki, Finland

Congenital nephrotic syndrome of the Finnish type (NPHS1) is associated with the rapid development of glomerular and tubulointerstitial fibrosis. Here we measured morphologic and molecular changes in the peritubular capillaries of the kidney in patients with NPHS1. Immunohistochemical analysis for the endothelial cell marker CD31 showed marked narrowing and a moderate but significant reduction in peritubular capillary density, especially in areas of increased collagen I and α-smooth muscle actin content. No evidence of endothelial-mesenchymal transformation was found. There was increased expression (up to 43-fold) of hypoxia inducible factor-1α suggesting tubulointerstitial hypoxia. Double-labeling for CD31 and vimentin showed small foci of peritubular capillary loss and tubular cell damage. While the amount of intercellular adhesion molecule-1 was upregulated in endothelial cells, other adhesion molecules were only modestly expressed. Vascular endothelial growth factor expression was reduced by up to half and decreased endothelial progenitor cell marker CD34 expression indicated lack of vascular repair. Our results suggest that hypoxia in the tubulointerstitium caused by hypoperfusion of glomerular and tubulointerstitial capillaries and rarefaction of the latter may be important for the rapid progression of fibrosis in the kidneys of patients with NPHS1.

Kidney International (2009) **75,** 1099–1108; doi:10.1038/ki.2009.41; published online 18 February 2009

KEYWORDS: endothelial cells; nephrotic syndrome; NPHS1; peritubular capillaries; proteinuria; tubulointerstitial microvasculature

Correspondence: *Anne Kaukinen, Hospital for Children and Adolescents, University of Helsinki, Helsinki 00029, Finland.*
E-mail: anne.kaukinen@helsinki.fi

Received 7 June 2008; revised 2 December 2008; accepted 6 January 2009; published online 18 February 2009

Congenital nephrotic syndrome of the Finnish type (NPHS1) is a genetic disorder caused by mutations in the *NPHS1* gene encoding for nephrin, which is a podocyte-specific protein located at the slit diaphragm of kidney glomerulus.[1,2] In NPHS1, heavy proteinuria and podocyte foot process effacement are present at birth, and progressive glomerular and tubulointerstitial fibrosis develop during infancy.[3–6] Although the NPHS1 glomeruli show early mesangial expansion and narrowing of the glomerular capillaries, the structure of the glomerular endothelium is quite well preserved in kidneys removed at infancy.[6,7] Besides fibrosis, inflammation around glomeruli and oxidative stress has been the prominent findings in the tubulointerstitium of NPHS1 kidneys.[5]

Recent studies have suggested that tubulointerstitial microvasculature has an important role in the progression of renal diseases and chronic transplant nephropathy.[8–12] The injury and loss of peritubular capillaries (PTCs) result in impairment of oxygen and nutrient delivery to the tubules and interstitial cells, correlating with fibrosis and tubular atrophy.[13–16] Chronic hypoxia in the interstitium and tubuli has been suggested as a final common pathway to end-stage renal failure.[17,18] Most of these data come from animal models, and less information is available from human kidney diseases.[19–21]

In this work, we were interested in the possible signs of injury and loss of PTCs in NPHS1 kidneys removed at infancy. These kidneys serve as a unique human model for studies on the pathology of proteinuric kidney diseases. We studied the relationship of PTC network and interstitial fibrosis as well as endothelial inflammatory response, thrombi formation, and angiogenesis in PTCs of NPHS1 kidneys.

RESULTS

The histopathology in the NPHS1 kidneys nephrectomized in infancy was mostly normal with intact tubuli and glomeruli showing only slightly expanded mesangium. However, sclerotic glomeruli surrounded by inflammatory cell infiltrates, tubular dilatation, interstitial fibrosis, and obliterating arteries were observed with advancing age (Figure 1).

Rarefaction of PTCs

In areas with well-preserved histology, the peritubular space and capillaries (PTC) were narrow (Figure 1), which was clearly visualized using immunohistochemical staining for the endothelial cell marker CD31 (Figures 1 and 2). The density of PTCs was evaluated by calculating the area fraction (%) of CD31-positive PTCs in NPHS1 kidneys. In the NPHS1 kidneys with mild changes the CD31 expression was slightly reduced (0.073%/tubulus) compared with control group 1 kidneys (0.085%/tubulus; adult nephrectomized

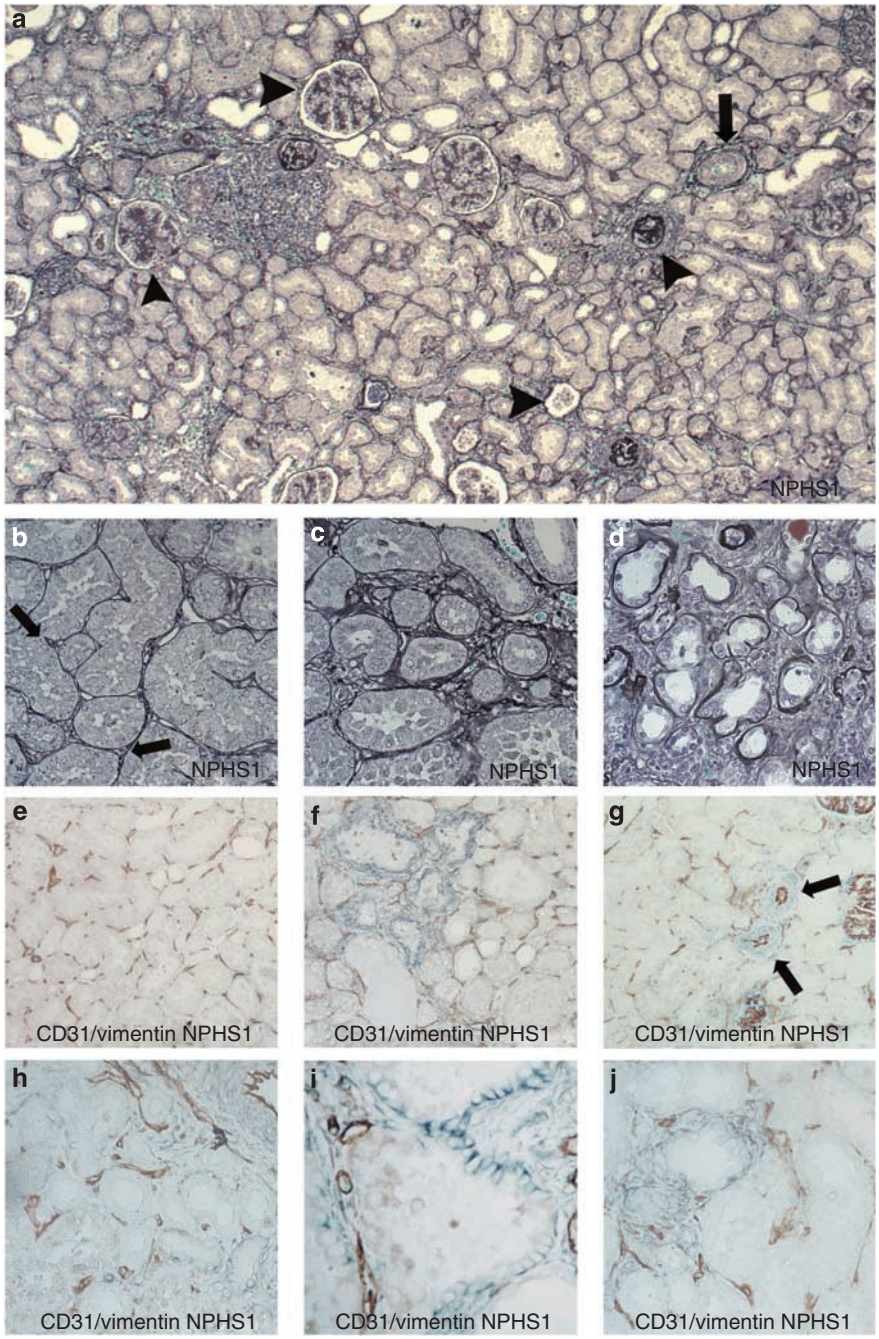

Figure 1 | Histological lesions and PTCs in NPHS1 kidneys. (**a**) A low-magnification image (× 50) of a NPHS1 kidney removed at the age of 8 months shows glomeruli with variable degrees of mesangial expansion and sclerosis. Sclerotic glomeruli are surrounded by inflammatory cells (arrowheads). The arterioles are typically narrowed (arrow) and the tubuli are well preserved, although some dilatation is evident (periodic acid silver methenamin staining). (**b**) Higher magnification image (× 400) shows oedemic tubuli and narrowed peritubular space and capillaries (arrows). (**c** and **d**) Focal increase of peritubular fibrosis occurs with time. (**e**) The NPHS1 kidneys with well preserved histology show regular staining of the endothelial cell marker CD31 (brown) and little vimentin expression (blue). (**f**) Focal increase of vimentin expression is, however, an early event and is associated with reduced staining for CD31. (**g**) Double staining for CD31 and vimentin shows clearly narrowed arterioles (arrows). (**h**–**j**) The expression of vimentin in peritubular space and tubuli is associated with reduced amount of CD31 staining, indicating a relationship with tubular damage and PTC rarefaction. NPHS1, congenital nephrotic syndrome of the Finnish type; PTC, peritubular space and capillaries.

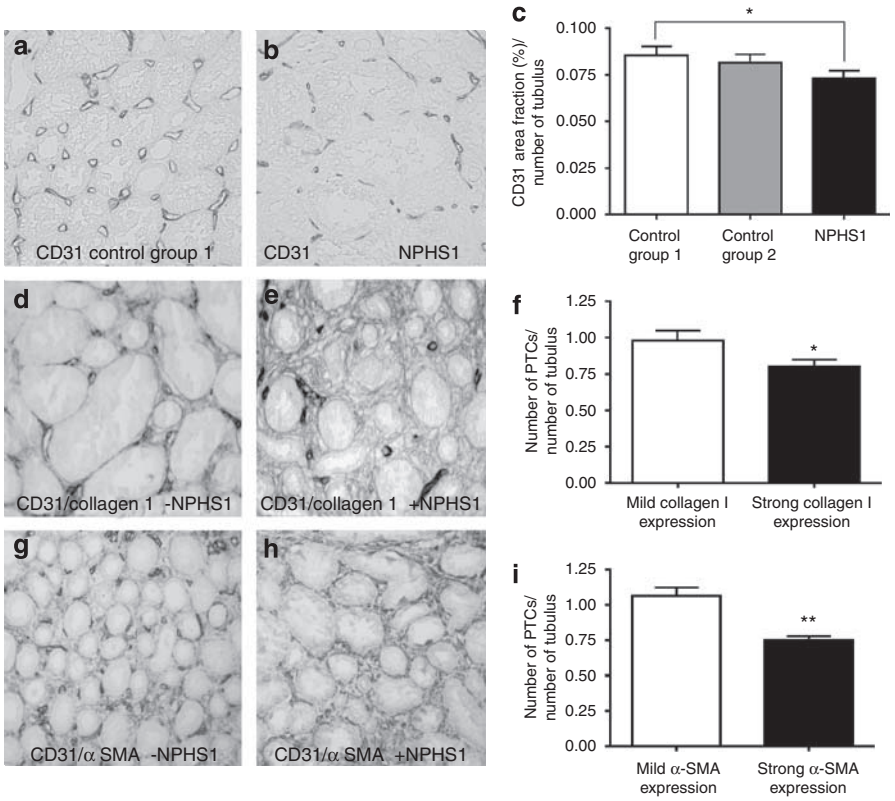

Figure 2 | The number of PTCs was reduced in NPHS1 kidneys. (**a** and **b**) Immunohistochemical staining for endothelial cell marker CD31 was used to visualize the PTC structures in control and NPHS1 kidneys. (**c**) The reduction of CD31 expression per number of tubulus was observed in NPHS1 samples. (The number of visual fields analyzed: 103 in control group 1, 39 in control group 2, and 42 NPHS1 samples). (**d**–**i**) The number of PTCs was decreased in NPHS1 samples with strong expression (+) of collagen I (number of visual fields analyzed; 92) and α-SMA (number of visual fields analyzed; 95) when compared with samples with mild expression of (−) of collagen I and α-SMA. (Original magnification × 200) *$P<0.05$, **$P<0.01$.

kidneys) ($P<0.05$) and control group 2 kidneys (0.082%/ tubulus; biopsy samples from proteinuric pediatric kidneys) (*P*-value not significant) (Figure 2a–c). The association of PTC density with interstitial changes was studied by counting the CD31-positive PTC cross-sections per tubulus in areas without and with peritubular collagen I staining. In the NPHS1 kidneys, the number of PTCs decreased from 0.982/ tubulus (no fibrosis) to 0.800/tubulus ($P<0.05$) (fibrosis) (Figure 2d–f). The PTC number per tubulus in control group 2 was 0.892 (*P*-value NS). Similarly, the number of PTCs per tubulus was 1.064 in areas with little expression of α-smooth muscle actin (α-SMA) as compared with 0.749 in areas with high α-SMA expression ($P<0.01$) (Figure 2g–i). Possible transformation of PTC endothelial cells to mesencymal cell was studied by double immunofluorescence staining for CD31 and α-SMA. The analysis of 96 visual fields in NPHS1 kidneys, however, did not show costaining of these two markers (Figure 3a and b).

Increased expression of vimentin in the peritubular space was an early event in NPHS1 kidneys. Double staining for CD31 and vimentin showed that in NPHS1 kidneys vimentin stained strongly both in endothelial cells and outside PTCs, whereas in control kidneys vimentin expression was modest and restricted to the endothelial cells (Figure 3c and d). Interestingly, vimentin expression was associated with small foci of PTC loss and tubular damage (Figure 1h–j).

Double staining of the two endothelial cell markers CD31 and CD34 gave a very similar pattern. As CD34 is also a marker for endothelial/hematopoietic progenitor cells, which possibly play a role in the healing of microvasculature, we searched especially capillaries and cells strongly positive for CD34 but less positive for CD31. Analysis of NPHS1 kidneys showed one cellular focus in every sixth visual field (25/151), but these were mostly present among cell infiltrates (Figure 3e–h) speaking against a decisive role of CD34-positive cells in the maintenance of PTCs.

Endothelial cell adhesion molecules and their ligands

Upregulation of endothelial adhesion molecules and selectins is believed to be important in triggering inflammatory and fibrotic processes in kidneys. The expression of adhesion molecules and their ligands was studied by immunohistochemistry and PCR microarray. Overall, the expression of adhesion molecules in PTCs of NPHS1 kidneys was moderate (Figure 4a–e and j). The staining intensity for intercellular adhesion molecule-1 (ICAM-1) was 1.5 times ($P<0.01$) higher in NPHS1 kidneys as compared with control group 1, whereas its expression was equal to control group 2.

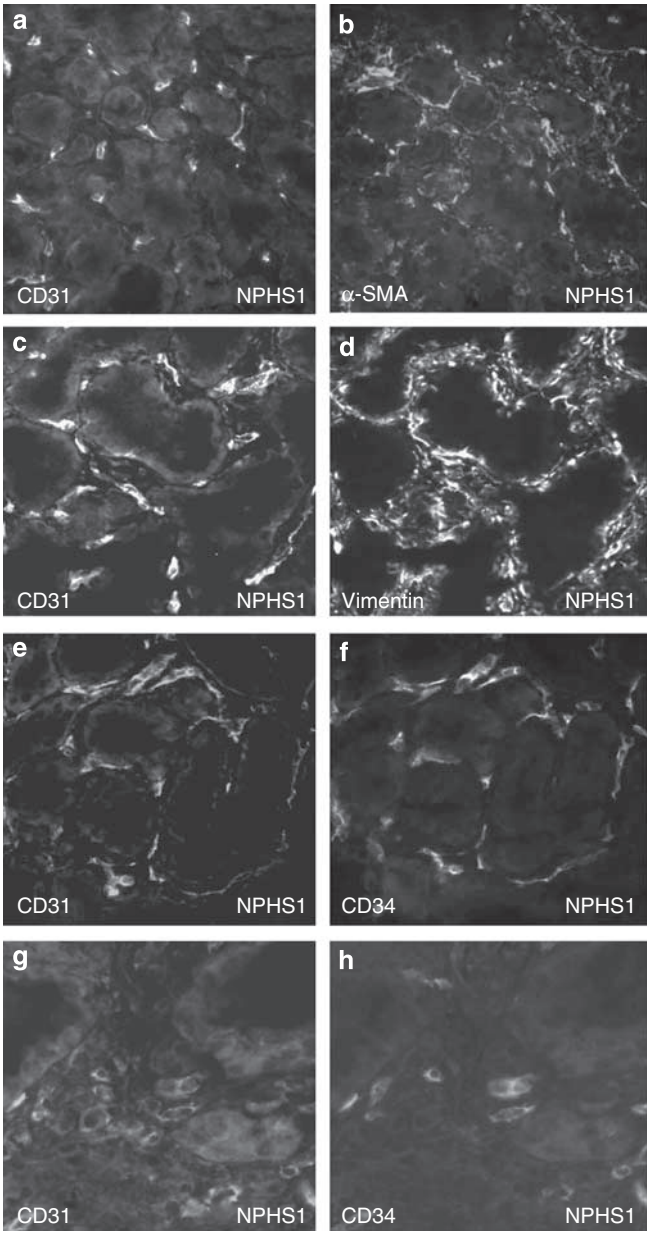

Figure 3 | Double stainings of CD31 with α-SMA, vimentin, and CD34. (**a** and **b**) Possible transformation of PTC endothelial cells to mesencymal cell was studied by double IF staining for CD31 and α-SMA. The analysis of 96 visual fields in NPHS1 kidneys, however, did not reveal costaining of these two markers. (**c** and **d**) Double staining for CD31 and vimentin showed strong and early expression of vimentin both in PTC endothelium and in the surrounding peritubular space. (**e** and **f**) The expression of CD31 and CD34 was mostly colocalized in endothelial cells. (**g** and **h**) Small foci with stronger expression of CD34 were seen among the cellular infiltrates. (Original magnification × 400).

P-selectin expression was 2.1 (*P*-value NS) higher in NPHS1 kidneys as compared with control group 1. Surprisingly, very little expression of vascular cell adhesion molecule-1 (VCAM-1) and E-selectin (endothelial leukocyte adhesion molecule-1) was detected. Also, the staining for CD29 (β1-integrin) was faint in control group 1 and NPHS1 kidneys. The mRNA levels of the adhesion molecules were also moderate showing upregulation of fibronectin, selectin L, and VCAM-1 (Figure 5a).

In the peritubular space, the number of inflammatory cells expressing the ligands for the endothelial adhesion molecules varied (Figure 4f–i and k). The expression levels of leukocyte function antigen-1 were 2.1 ($P<0.01$) and 3.3 (*P*-value NS) times higher in NPHS1 kidneys as compared with control groups 1 and 2, respectively. The correlation was observed in the expression of ICAM-1 and its ligand leukocyte function antigen-1 in all six individual patient samples. The expression levels of P-selectin glycoprotein ligand-1 were 4.7 ($P<0.01$) and 2.3 (*P*-value NS) times higher in NPHS1 kidneys as compared with control groups 1 and 2, respectively. For very late antigen-4 the numbers were 3.2 (*P*-value NS) and 2.8 (*P*-value NS). In the PCR microarray, the mRNA-levels of P-selectin glycoprotein ligand were clearly upregulated (Figure 5a).

Markers for hypoxia, thrombosis, and angiogenesis

The progression of tubulointerstitial injury in various renal diseases is associated with chronic hypoxia. In NPHS1 kidneys, the hypoxia-inducible factor-1α (HIF-1α) was detected around tubuli as positive nuclear staining and the protein expression was 2.6 ($P<0.05$) and 43 ($P<0.01$) times more prevalent in NPHS1 kidneys as compared with control groups 1 and 2, respectively (Figure 6a–d). HIF-1α was also upregulated in NPHS1 cortex lysates in western blot analysis (Figure 6i and j). The expression was approximately two times higher in NPHS1 cortex than in samples of control group 1. Vascular endothelial growth factor (VEGF) was mostly expressed (in addition to glomeruli) in tubuli showing a diffuse cytoplasmic or an apical staining pattern (Figure 6e–g). Somewhat surprisingly VEGF expression in NPHS1 kidneys was decreased by 30% (*P*-value NS) and 52% ($P<0.01$) when compared with control groups 1 and 2, respectively (Figure 6h). Both western blot analysis and the PCR microarray of the kidney cortex samples showed equal reduction in the VEGF expression (Figures 5c, 6i and j). The overall profile of the angiogenic molecules in the microarray showed neither up- nor downregulation of the VEGF-related molecules (Figure 5c).

In the NPHS1 kidneys, heavy proteinuria and dyslipidemia lead to arteriolar obliteration already visible in kidneys removed at infancy (Figure 1). The possible role of thrombotic events in PTCs was evaluated by direct microscopy (Herowitc staining) but it did not show thrombi in PTC. Also, staining for a prothrombotic vonWillebrand factor and the platelet marker CD61 did not indicate thrombus formation in PTCs (Figure 7a–c). Interestingly, the staining pattern of fibrin in PTCs of NPHS1 kidneys showed great variation from sample to sample (Figure 7d and e). Fibrin staining was not detected in samples of control group 2 (Figure 7f).

DISCUSSION

We examined morphological and molecular changes of PTCs in NPHS1 kidneys. In this disease, mutations in

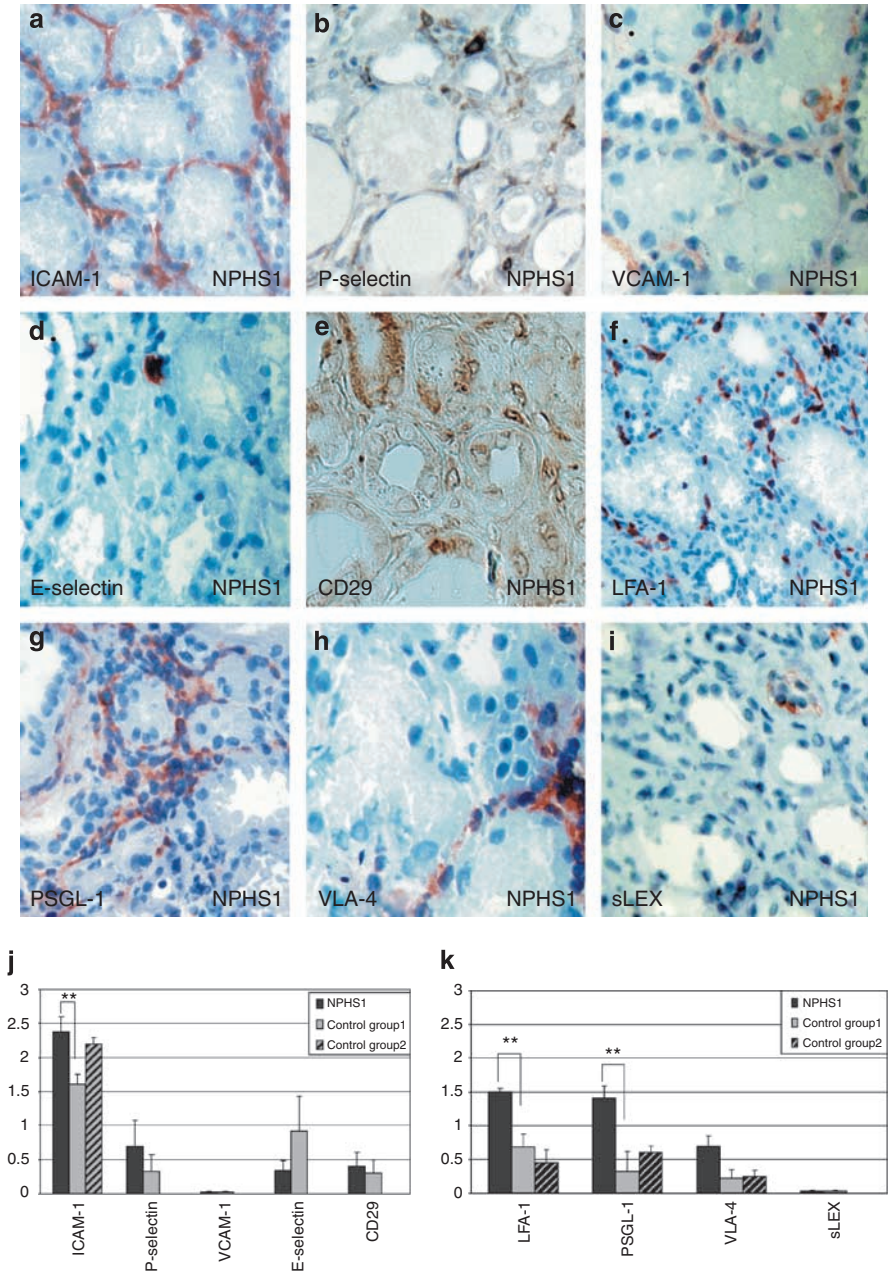

Figure 4 | The expression of adhesion molecules and their ligands in peritubular space of NPHS1 kidneys. (**a**) The staining intensity for ICAM-1 was 1.5 times ($P<0.01$) higher in NPHS1 kidneys as compared with control group 1, whereas its expression was equal to control group 2. (**b**) The expression of P-selectin was modest, although higher ($\times$ 2.1) than in controls. (**c**–**e**) Peritubular expression of VCAM-1, E-selectin (ELAM-1), and CD29 (β1-integrin) was very modest. (**f**–**h**) The expression levels of LFA-1 (ligand for ICAM-1), PSGL-1 (ligand for P-selectin), and VLA-4 (ligand for VCAM-1) were higher in NPHS1 kidneys as compared with control groups 1 and 2. (**j** and **k**) The results are presented as an average of PTC-positive foci per visual field. (Original magnification $\times$ 400) $^{**}P<0.01$.

podocyte-specific nephrin affect only glomeruli, and the interesting question is how the glomerular injury is transmitted to tubulointerstitium leading to renal fibrosis. Our results suggest that hypoperfusion and injury in glomerular and PTCs may result in interstitial hypoxia and fibrosis as well as tubular damage.

Chronic hypoxia is regarded as a major factor contributing to the development of renal fibrosis.[18] PTCs are essential for supplying oxygen to the tubular system and their role has recently been emphasized both in renal diseases and chronic allograft nephropathy.[14,22,23] In our study, increased amount of HIF-1α was found in the tubulointerstitium of NPHS1 kidneys implicating low oxygen tension. The most probable explanation for this was hypoperfusion in PTCs, caused by the obliteration of the atherosclerotic arterioles, glomerular capillaries, and PTCs, as observed in this work and our previous studies.[6,7] Mesangial expansion and glomerular capillary obliteration develop early in NPHS1 kidneys

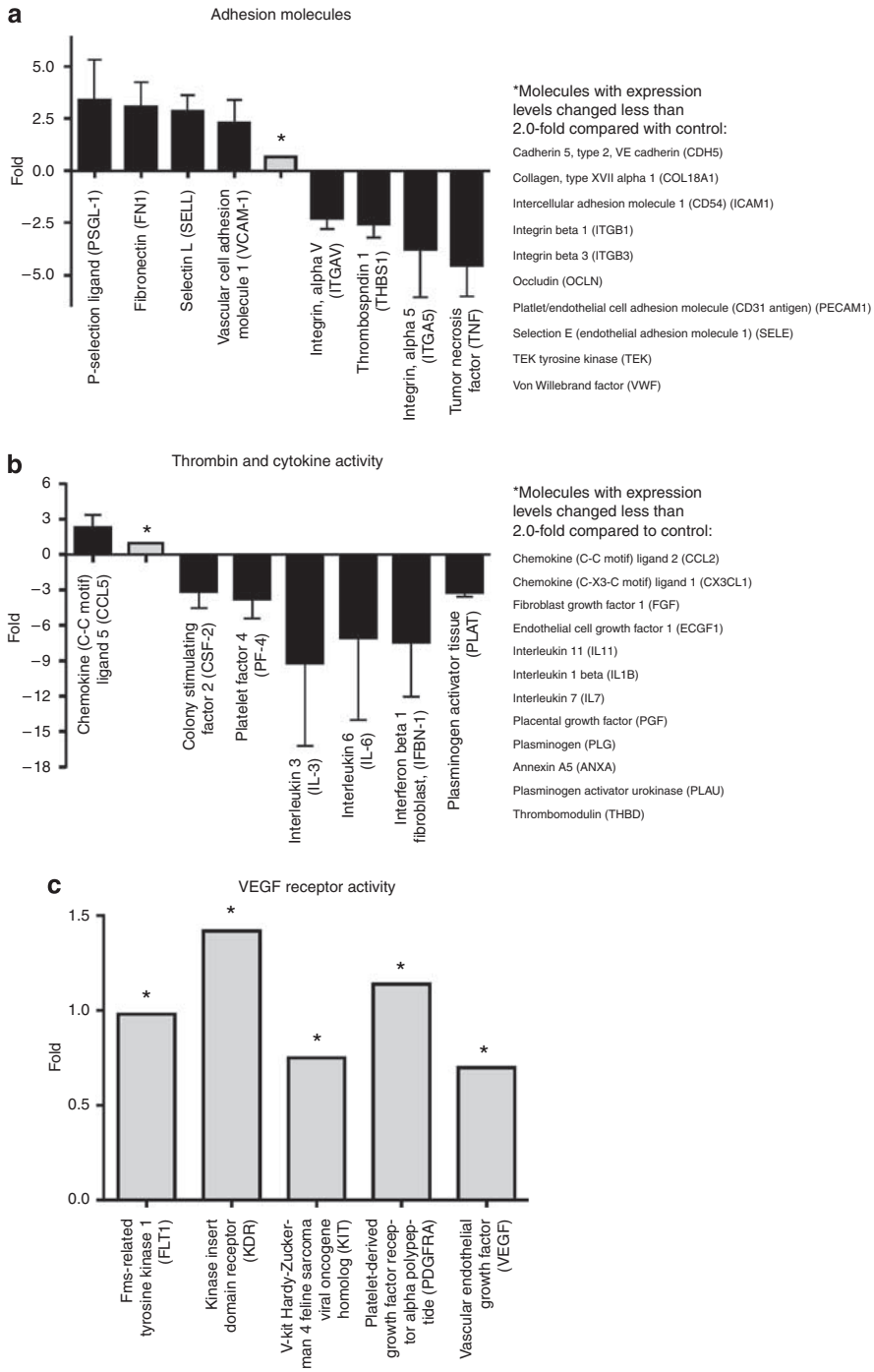

Figure 5 | The analysis of real-time reverse transcription–PCR from NPHS1 kidney cortex. (**a**–**c**) The analysis was carried out for important adhesion molecules, cytokines, and molecules related to thrombin activity and VEGF receptor molecules. The results are presented as fold of mRNA changes in NPHS1 samples compared with control samples. The array was carried out in triplicate from each three NPHS1 patient samples.

reducing circulations in PTCs, which reside downstream to glomeruli. Swelling and dilatation of the tubuli due to massive proteinuria also favours hypoperfusion in PTCs. Whether vascular thrombi in PTCs were an additional factor in tubulointerstitial ischemia was evaluated by the immunohistochemical studies on the platelet marker CD61. Only a few CD61-positive foci, however, were observed indicating a minor role for the thrombus formation in PTCs.

Loss of PTCs was clearly associated with the development of interstitial fibrosis (collagen I expression) and appearance of myofibroblasts (α-SMA expression). Hypoxia is known to induce transformation of interstitial fibroblasts into myofibroblast,[24,25] which seems as a possible trigger also in NPHS1 kidneys. Transformation of endothelial cells into myofibroblasts has also been recently suggested,[26,27] but double staining for CD31 and α-SMA did not show such foci in

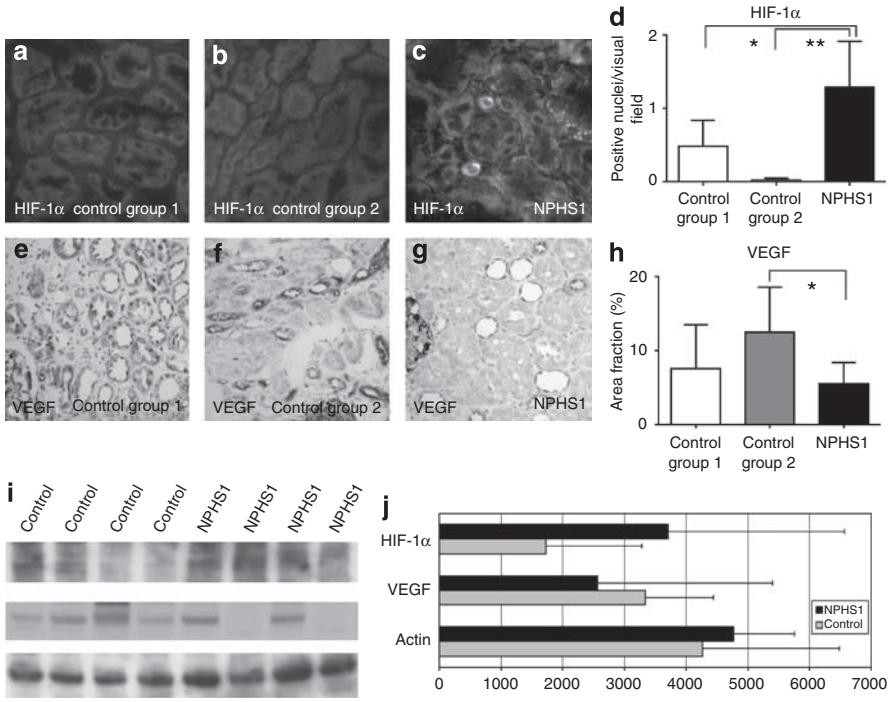

Figure 6 | The upregulation of HIF-1α was evident, whereas the expression of VEGF was slightly downregulated in NPHS1 kidneys. (**a**–**d**) Hypoxia-inducible factor 1α (HIF-1α) was detected around tubuli as positive nuclear staining and was 2.6 (control group 1) and 43 (control group 2) times more prevalent in NPHS1 kidneys as compared with controls. (**e**–**g**) VEGF was expressed (in addition to glomeruli) in tubuli showing a diffuse cytoplasmic or an apical staining pattern. (**h**) VEGF expression was decreased by 30% (control group 1) and 52% (control group 2) in NPHS1 kidneys. (**i** and **j**) HIF-1α was also upregulated in NPHS1 cortex lysates in western blot analysis. The expression was approximately two times higher in NPHS1 cortex than control samples. Western blot analysis of the kidney cortex samples showed the reduction in the VEGF expression. (Original magnification × 400) *$P < 0.05$.

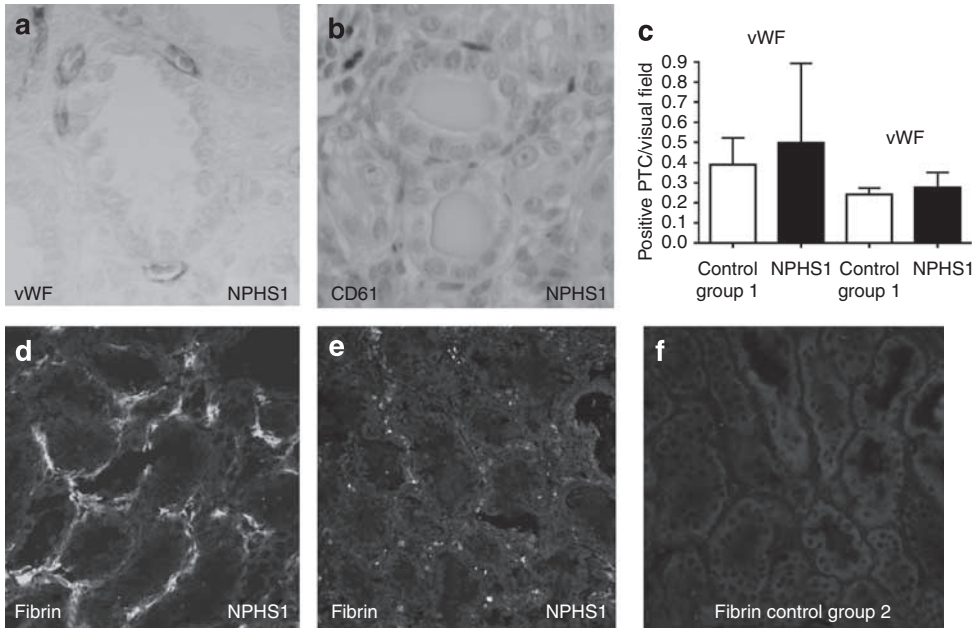

Figure 7 | PTCs in NPHS1 kidneys did not show any thrombus formation. (**a**–**c**) The stainings for a prothrombotic vonWillebrand factor (vWF) and the platelet marker CD61 did not indicate thrombus formation in PTCs of NPHS1 kidneys. (**d**–**f**) The staining pattern of fibrin in PTCs of NPHS1 kidneys showed great variation from sample to sample, whereas fibrin staining was not observed in control group 2 samples.

NPHS1 kidneys. Instead, we found an interesting association of PTCs and another cytoskeleton protein vimentin. In NPHS1 kidneys, vimentin was clearly an early marker for peritubular and tubular lesions, and double staining for CD31 and vimentin showed small foci with vimentin expression and loss of PTCs. Early vimentin expression has

recently been reported in some kidney disorders and renal transplants,[28–30] and the association of this with PTC loss seems interesting.

Besides hypoxia, proteinuria is an important factor in the development of renal fibrosis.[31,32] Filtered macromolecules may exert critical effects on tubular cells leading to tubulointerstitial injury, epithelial–mesenchymal transformation, and production of proinflammatory and profibrotic cytokines and chemokines.[33] Our previous studies indicated that tubular cells in the NPHS1 kidneys were quite resistant to proteinuria and showed little epithelial–mesenchymal transformation.[5] In this work, the cortical expression of mRNAs of several cytokines, such as interleukins and tumor necrosis factor, was lower in NPHS1 kidneys as compared with controls, and few inflammatory cells were found in the well preserved peritubular areas. Moreover, the mesangial expansion and periglomerular inflammation seemed to precede tubulointerstitial damage in the NPHS1 kidneys. These findings do not exclude the direct effects of proteinuria on the tubulointerstitium but suggest that hypoperfusion is an important factor for the development of interstitial fibrosis. These data are in agreement with the recent findings by Wong *et al.*,[34] who found that reduction of parent glomerular capillaries and hypoxic insults more strongly influenced PTC flow and tubulointerstitial damage than proteinuria alone in a model of subacute renal disease.

The PTC injury may result in endothelial activation with enhancement of inflammation and thrombotic events.[35,36] High plasma cholesterol and triglyceride levels may also induce endothelial dysfunction in severely nephrotic NPHS1 patients.[37] Adhesion molecules propagate the inflammatory response and facilitate the adherence of leukocytes to the microvascular endothelium.[38] Our results on the expression of adhesion molecules and their ligands were mixed. Although strong expression of ICAM-1 was evident in the PTCs of NPHS1 kidneys, the expression of P-selectin, VCAM-1, and E-selectin was quite weak in the immunostaining. Also, the pattern of mRNA expression in the PCR microarray did not show uniform activation of adhesion molecules. ICAM-1 is the main endothelial ligand for β2-integrin and it is involved in the transmigration of lymphocytes and neutrophils expressing leukocyte function antigen-1, which was also upregulated in NPHS1 kidneys.[39] Elevated ICAM-1 levels have also been reported in other nephrotic disorders but its role in these non-inflammatory disorders remains open.[40–42] Somewhat surprisingly, the expression of VCAM-1, which binds to β1-integrins and, in addition to leukocyte recruitment, is involved in atherosclerotic processes, was very low in NPHS1 kidneys.[43]

Angiogenesis is believed to be an important mechanism in the maintenance of vascular integrity in the ischemic and inflammatory renal disorders.[44] Local production of angiogenesis factors, proliferation of endothelial cells, and recruitment of endothelial progenitor cells are involved in the repair process. On the basis of this, it was surprising that the expression of the major angiogenesis factor VEGF was low in NPHS1 kidneys as studied by immunohistochemistry, western blotting, and PCR microarray. Also, the PCR microarray did not show upregulation of mRNAs of VEGF receptors. Moreover, the expression level of β1-integrins, that are believed to be involved in angiogenesis,[45] was low in immunostaining and PCR microarray. These data are in contrast to some animal models[46] but they are in agreement with the recent results of Lindenmeyer *et al.*,[47] who found reduced VEGF expression in the tubulointerstitium of human diabetic kidneys with interstitial vascular rarefaction. The possible role of endothelial progenitor cells in vascular repair was studied by double staining for the endothelial progenitor cell markers CD34 and CD31 (mature endothelial cells). The stainings, however, did not show vascular structures with high CD34 and low CD31 expression. These data indicate that the reparative capability of NPHS1 kidneys is limited, which fits to the fast progression of fibrosis.

The NPHS1 kidneys, nephrectomized at an early stage when renal function still is quite normal, serve as a unique model for studies on the pathophysiology of nephrotic kidney diseases. The problem is that it is not possible to obtain normal age-matched kidney material (not showing dysplasia or cellular damage caused by cytotoxic drugs). Therefore, tissue samples from adult kidneys with normal histology and function (control group 1) and biopsies from children, aged 2–14 years, who suffered from proteinuric disorders (mostly minimal change nephrotic syndrome) (control group 2) was used as controls. So, caution is warranted in the interpretation of the results dealing with the expression levels of some molecular markers. Most of the data on NPHS1 kidneys presented is, however, valid without optimal controls. This is especially the case with the histological findings and the expression of many markers (abundant vs little expression).

In conclusion, hypoperfusion of PTCs and tubulointerstitial hypoxia were evident in NPHS1 kidneys. Vimentin expression was an early marker for tubulointerstitail lesions associated with the PTC loss. The inflammatory response of PTCs was seen as an upregulation of ICAM-1 expression. Endothelial–mesenchymal transformation was not observed and, based on the analysis of angiogenesis factors and the CD34 expression, vascular repair of PTCs was modest.

MATERIALS AND METHODS

Kidney tissue samples

The kidney samples came from 44 children with NPHS1 (age 3–44 months), nephrectomised at the Hospital for Children and Adolescents, University of Helsinki, Finland in 1986–2006. The genotypes of the NPHS1 patients were as follows: Fin-major homozygotes 32 patients, Fin-major/Fin-minor compound heterozygotes 5 patients, Fin-minor homozygotes 3 patients, and Fin-major/missense mutation 4 patients. We did not find any association with the genotype and the pathological findings. Routine formalin-fixed and paraffin-embedded samples were prepared, and the rest of the renal cortex was snap-frozen in liquid nitrogen and stored at −70 °C. All patients had severe nephrotic syndrome from the birth and were treated with daily albumin infusions to supplement the

continuous heavy protein losses. As a control group 1 we used 10 normal adult kidneys (age 47–58 years) removed for transplantation. These kidneys had proved unsuitable for transplantation mainly because of vascular abnormalities. Control group 2 consisted of biopsies from 14 children (age 2–14 years). Ten of these patients suffered from minimal change nephrotic syndrome (U-Prot values: 22, 63, 133, 984, 554, 53, 70, 5170, 803, and 3170 mg/l at the time of biopsy), three patients suffered from focal segmental glomerulosclerosis (U-Prot values: 132, 2310, and 3220 mg/l), and one patient had mesangioproliferative glomerulonefritis (U-Prot value: 2510 mg/l).

Antibodies

Antibodies used for immunofluorescence stainings included mouse monoclonal antibodies against CD34 (Dako Cytomation, Glostrup, Denmark), fibrin (Santa Cruz Biotechnology Inc., Santa Cruz, CA, USA), HIF-1α (BD Transduction Laboratories, San Jose, CA, USA), human SMA (Dako Cytomation, Glostrup, Denmark), and vimentin (Dako Cytomation). Antibodies for immunofluorescence included also rabbit polyclonal antibody against platelet endothelial cell adhesion molecule-1 (CD31) (Novus Biologicals Inc., Littleton, CO, USA).

Antibodies for immunoperoxidase stainings included mouse monoclonal antibodies against CD29 (Visionbiosystems novocastra, Newcastle upon Tyne, UK), CD61 (Dako Cytomation), CD34 (Dako Cytomation), collagen I (Acris Antibodies, Hiddenhausen, Germany), endothelial leukocyte adhesion molecule (ELAM-1, E-selectin, CD62E) (R&D Systems, Minneapolis, MN, USA), human SMA (Dako Cytomation), intercellular adhesion molecule-1 (ICAM-1, CD54) (R&D Systems), leukocyte function antigen-1 (LFA-1, CD11a) (Dako Cytomation), platelet endothelial cell adhesion molecule-1 (PECAM-1, CD31) (Dako Cytomation), P-selectin glycoprotein ligand (PSGL-1, CD162) (Santa Cruz Biotechnology Inc.), Sialyl-LewisX (sLEX, CD15s) (BD Pharmingen, San Jose, CA, USA), vascular cell adhesion molecule-1 (VCAM-1, CD106) (R&D Systems), very late antigen-4 (VLA-4, CD49d) (Serotec, Oxford, UK). Antibodies for immunoperoxidase stainings also included goat polyclonal antibody against P-selectin (Santa Cruz Biotechnology Inc.).

Microscopy and immunohistochemistry

The histological lesions in NPHS1 kidneys were evaluated by light microscopy from paraffin-embedded tissue sections stained with periodic acid silver methenamin.

Immunoperoxidase stainings were performed in a traditional way using sections of formalin-fixed, paraffin-embedded or snap-frozen, acetone-fixed cryosections (5 μm) of kidney tissue samples. In the immunoperoxidase staining of the cryosections, a peroxidase-conjugated rabbit anti-mouse (Dako, Copenhagen, Denmark) and peroxidase-conjugated goat anti-rabbit antibody (Zymed, San Franciso, CA, USA) were used as second antibodies. The reaction was revealed by 3-amino-9-ethyl carbazole solution containing hydrogen peroxide; Mayer's hemalum was used for counterstaining. When staining formalin-fixed, paraffin-embedded sections, microwave treatment in 10 mmol/l citric acid for 10 min was performed or Dako Target Retrieval Solution (S1699) (Dako Cytomation) was used to improve the antibody penetration. Amplification of the primary antibody reaction was achieved by incubating the sections with biotinylated secondary antibody (Vector Elite ABC Kit) (Vector Laboratories Inc., Burlingame, CA, USA) or TSA Indirect, tyramide signal amplification-kit (Perkin Elmer LAS Inc., NEL700). For the immunofluorescence stainings the cryosections (5 μm) of kidney samples were fixed with acetone or 3.5% paraformaldehyde, depending on the antibody used. The stainings were performed in a conventional way.[5]

Semiquatitative scoring system

Randomly selected visual fields from kidney interstitium sample were analyzed at $\times 400$ magnification in the light microscope for the following parameters: (1) Mean area fraction (%) of CD31-positive PTCs per number of tubuli in each visual field. Images were analyzed by NIH ImageJ 1.35p program (National Institutes of Health, USA) by calculating the area fractions of immunostained components. The proportion of black-to-white pixels in the image was calculated as percentage. (2) Mean number of CD31-positive PTCs per number of tubuli in each visual field. (3) The number of adhesion molecules, their ligands, and HIF-1α-positive PTCs were calculated and results are presented as positive foci per visual field.

Total RNA isolation and real-time reverse transcription–PCR

Total RNA from cortical tissues from control and NPHS1 patients was isolated with TRIzol Reagent (Invitrogen Life Technologies, Carlsbad, CA, USA) and further purified with Rneasy Mini Kit (QIAGEN, GmbH, Germany) according to the manufacturer's protocols. cDNA synthesis was carried out with an RT^2 PCR Array First Strand Kit (C-02) (SuperArray Bioscience Corporation, Frederick, MD, USA) by incubating 2 μg of isolated RNA at $+37\,^{\circ}C$ for 1 h. The synthesized cDNA was subjected to real-time PCR (ABI PRISM 7000; Applied Biosystems, Foster City, CA, USA) using RT^2 Real-Time SYBR Green/ROX PCR Master Mix (PA-112) (SuperArray Bioscience Corporation). The Human Endothelial Cell Biology RT^2 Profiler PCR Array (APHS-015A) (SuperArray Bioscience Corporation) was used to profile the expression of 84 genes related to endothelial cell biology. The PCR was amplified for 40 cycles. Each PCR was subjected to melting curve analysis. Threshold cycles for each primer were separately analyzed. The following equation was used to normalize the expression level of a gene of interest (GOI) to a housekeeping gene (HKG = β-actin) $= 2^{-[Ct(GOI)-Ct(HKG)]} = 2^{-\Delta Ct}$. To determine the gene expression profile in NPHS1 cortical tissues, the normalized expression of the GOI in the experimental sample (ΔC_t expt) was divided by the normalized expression of the same GOI in the control sample (ΔC_t control), where $\Delta\Delta C_t = \Delta C_t$ expt $- \Delta C_t$ control. Representative data are presented in terms of fold mRNA changes of NPHS1 samples compared with control samples.

Western blotting

The kidney cortex was homogenized with Ultra-Turrax (Rose Scientific Ltd, Alberta, Canada) in 0.08 M Tris-HCl pH 6.8 buffer containing 2% SDS and 10% glycerol. Western blotting was performed in a conventional way as previously described.[5] Antibodies for western blotting included anti-actin goat polyclonal antibody (Santa Cruz Biotechnology Inc.), anti-HIF-1α mouse monoclonal antibody (BD Transduction Laboratories), anti-VEGF mouse monoclonal antibody (Santa Cruz Biotechnology Inc.), donkey anti-goat IgG-HRP conjugated antibody (Santa Cruz Biotechnology Inc.), and goat anti-mouse IgG-HRP conjugated antibody (Santa Cruz Biotechnology Inc.).

Statistics

Data are presented as mean ± s.d. Two-tailed P-values < 0.05 (Student's t-test) were considered significant.

Ethics

The study was approved by the Ethics Committee of the Hospital for Children and Adolescents, University of Helsinki.

DISCLOSURE

All the authors declared no competing interests.

ACKNOWLEDGMENTS

This work was supported by grants from the Sigrid Juselius Foundation, the Pediatric Research Foundation, the Päivikki and Sakari Sohlberg Foundation, and Helsinki University Central Hospital Research Fund. We warmly thank Tuike Helmiö and Marjatta Palovaara for their excellent technical assistance. We also thank Dr Jouni Lauronen for help with patient data.

REFERENCES

1. Kestilä M, Lenkkeri U, Männikkö M *et al.* Positionally cloned gene for a novel glomerular protein-nephrin is mutated in congenital nephrotic syndrome. *Mol Cell* 1998; **1**: 575–582.
2. Ruotsalainen V, Ljungberg P, Wartiovaara J *et al.* Nephrin is specifically located at the slit diaphragm of glomerular podocytes. *Proc Natl Acad Sci USA* 1999; **96**: 7962–7967.
3. Patrakka J, Kestilä M, Wartiovaara J *et al.* Congenital nephrotic syndrome (NPHS1): features resulting from different mutations in Finnish patients. *Kidney Int* 2000; **58**: 972–980.
4. Lahdenkari A-T, Lounatmaa K, Patrakka J *et al.* Podocytes are firmly attached to glomerular basement membrane in kidneys with heavy proteinuria. *J Am Soc Nephrol* 2004; **15**: 2911–2918.
5. Kuusniemi A-M, Lapatto R, Holmberg C *et al.* Kidneys with heavy proteinuria show fibrosis, inflammation and oxidative stress, but no tubular phenotypic change. *Kidney Int* 2005; **68**: 121–132.
6. Kuusniemi A-M, Merenmies J, Lahdenkari AT *et al.* Glomerular sclerosis in kidneys with congenital nephrotic syndrome (NPHS1). *Kidney Int* 2006; **70**: 1423–1431.
7. Kaukinen A, Kuusniemi A-M, Lautenschlager I *et al.* Glomerular endothelium in kidneys with congenital nephrotic syndrome of the Finnish type. *Nephrol Dial Transplant* 2008; **23**: 1224–1232.
8. Nakagawa T, Kang DH, Ohashi R *et al.* Tubulointerstitial disease: role of ischemia and microvascular disease. *Curr Opin Nephrol Hypertens* 2003; **12**: 233–241.
9. Rodriguez-Iturbe B, Johnson RJ, Herrera-Acosta J. Tubulointerstitial damage and progression of renal failure. *Kidney Int* 2005; **99**(Suppl): S82–S86.
10. Ivanyi B, Fahmy H, Brown H *et al.* Peritubular capillaries in chronic renal allograft rejection: a quantitative ultrastructural study. *Human Pathol* 2000; **31**: 1129–1138.
11. Ohashi R, Kitamura H, Yamanaka N. Peritubular capillary injury during the progression of experimental glomerulonephritis in rats. *J Am Soc Nephrol* 2000; **11**: 47–56.
12. Kang DH, Kanellis J, Hugo C *et al.* Role of the microvascular endothelium in progressive renal disease. *J Am Soc Nephrol* 2002; **13**: 806–816.
13. Rabelink TJ, Wijewickrama DC, de Koning EJ. Peritubular endothelium: the Achilles heel of the kidney. *Kidney Int* 2007; **72**: 926–930.
14. Norman JT, Fine LG. Intrarenal oxygenation in chronic renal failure. *Clin Exp Pharmacol Physiol* 2006; **33**: 989–996.
15. Eddy AA. Can renal fibrosis be reversed? *Pediatr Nephrol* 2005; **20**: 1396–1475.
16. Choi YJ, Chakraborty S, Nguyen V *et al.* Peritubular capillary loss is associated with chronic tubulointerstitial injury in human kidney: altered expression of vascular endothelial growth factor. *Human Pathol* 2000; **31**: 1491–1497.
17. Nangaku M. Chronic hypoxia and tubulointerstitial injury: a final common pathway to end-stage renal failure. *J Am Soc Nephrol* 2006; **17**: 17–25.
18. Nangaku M. Hypoxia and tubulointerstitial injury: a final common pathway to end-stage renal failure. *Nephron Exp nephrology* 2004; **98**: e8–e12.
19. Shu Y, Hoshi S, Tomari S *et al.* Phenotypic changes and cell cycle activation in early tubulointerstitial injury of rat adriamycin nephrosis. *Pathol Int* 2002; **52**: 214–223.
20. Gandhi M, Olson JL, Meyer TW. Contribution of tubular injury to loss of remnant kidney function. *Kidney Int* 1998; **54**: 1157–1165.
21. Benigni A, Gagliardini E, Remuzzi A *et al.* Angiotensin-converting enzyme inhibition prevents glomerular-tubule disconnection and atrophy in passive Heymann nephritis, an effect not observed with a calcium antagonist. *Am J Pathol* 2001; **159**: 1743–1750.
22. Basile DP. Rarefication of peritubular capillaries following ischemic acute renal failure: a potential factor predisposing to progressive nephropathy. *Curr Opin Nephrol Hypertens* 2004; **13**: 1–7.
23. Ishii Y, Sawada T, Kubota K *et al.* Injury and progressive loss of peritubular capillaries in the development of chronic allograft nephropathy. *Kidney Int* 2005; **67**: 321–332.
24. Muchaneta-Kubara EC, El Nahas AM. Myofibroblast phenotypes expression in experimental renal scarring. *Nephrol Dial Transplant* 1997; **12**: 904–915.
25. Manotham K, Tanaka T, Matsumoto M *et al.* Transdifferentation of cultured tubular cells induced by hypoxia. *Kidney Int* 2004; **65**: 871–880.
26. Simonson MS. Phenotypic transitions and fibrosis in diabetic nephropathy. *Kidney Int* 2007; **71**: 846–854.
27. O'Riordan E, Mendelev N, Patschan S *et al.* Chronic NOS inhibition actuates endothelial-mesenchymal transition. *Am J Physiol Heart Circ Physiol* 2007; **292**: H285–H294.
28. Sanai T, Sobka T, Johnson T *et al.* Expression of cytoskeletal proteins during the course of experimental diabetic nephropathy. *Diabetologia* 2000; **43**: 91–100.
29. Suzuki T, Kimura M, Asano M *et al.* Role of atrophic tubules in development of interstitial fibrosis in microembolism-induced renal failure in rat. *Am J Pathol* 2001; **158**: 75–80.
30. Hertig A, Anglicheau D, Verine J *et al.* Early epithelial phenotypic changes predict graft fibrosis. *J Am Soc Nephrol* 2008; **23**: 1–8.
31. de Zeeuw D, Remuzzi G, Parving HH *et al.* Proteinuria, a target for renoprotection in patients with type 2 diabetic nephropathy: lessons from RENAAL. *Kidney Int* 2004; **65**: 2309–2320.
32. Tarver-Carr M, Brancati F, Eberhardt MS *et al.* Proteinuria and the risk of chronic kidney disease (CDK) in the United States. *J Am Soc Nephrol* 2000; **11**: 168A.
33. Abbate M, Zoja C, Remuzzi G. How does proteinuria cause progressive renal damage? *J Am Soc Nephrol* 2006; **17**: 2974–2984.
34. Wong MG, Suzuki Y, Tanifuji C *et al.* Peritubular ischemia contributes more to tubular damage than proteinuria in immune-mediated glomerulonephritis. *J Am Soc Nephrol* 2008; **19**: 290–297.
35. Steeber DA, Guglielmo M, Venturi F *et al.* A new twist to the leukocyte adhesion cascade: intimate cooperation is key. *Trends Immunol* 2005; **26**: 9–12.
36. Tesfamariam B, DeFelice AF. Endothelial injury in the initiation and progression of vascular disorders. *Vascul Pharmacol* 2007; **46**: 229–237.
37. Trevisan R, Dodesini AR, Lepore G. Lipids and renal disease. *J Am Soc Nephrol* 2006; **17**: S145–S147.
38. Kakkar AK, Lefer DJ. Leukocyte and endothelial adhesion molecule studies in knockout mice. *Curr Opin Pharmacol* 2004; **4**: 154–158.
39. Hordijk PL. Endothelial signalling events during leukocyte transmigration. *FEBS J* 2006; **273**: 4408–4415.
40. Muller GA, Markovic-Lipkovski J, Muller CA. Intercellular adhesion molecule-1 expression in human kidneys with glomerulonephritis. *Clin Nephrol* 1991; **36**: 203–208.
41. Dal Canton A, Fuiano G, Sepe V *et al.* Mesangial expression of intercellular adhesion molecule-1 in primary glomerulosclerosis. *Kidney Int* 1992; **41**: 951–955.
42. Wuthrich RP, Jevnikar AM, Takei F *et al.* Intercellular adhesion molecule-1 (ICAM-1) expression is upregulated in autoimmune murine lupus nephritis. *Am J Pathol* 1990; **136**: 441–450.
43. Seron D, Cameron JS, Haskard DO. Expression of VCAM-1 in the normal and diseased kidney. *Nephrol Dial Transplant* 1991; **6**: 917–922.
44. Reinders MEJ, Rabelink TJ, Briscoe DM. Angiogenesis and endothelial cell repair in renal disease and allograft rejection. *J Am Soc Nephrol* 2006; **17**: 932–942.
45. Mettouchi A, Meneguzzi G. Distinct roles of β1 integrins during angiogenesis. *Eur J Cell Biol* 2006; **85**: 243–247.
46. Schrijvers BF, Flyvbjerg A, De Vriese AS. The role of vascular endothelial growth factor (VEGF) in renal pathophysiology. *Kidney Int* 2004; **65**: 2003–2017.
47. Lindenmeyer MT, Kretzler M, Boucherot A *et al.* Interstitial vascular rarefication and reduced VEGF-A expression in human diabetic nephropathy. *J Am Soc Nephrol* 2007; **18**: 1765–1776.